Volume 1 | Number 1 | Jan 2013 | Pages 1–100

## Journal of
## Materials Chemistry A

Materials for energy and sustainability
www.rsc.org/materialsA

Li⁺

ROYAL SOCIETY OF CHEMISTRY

ROYAL SOCIETY OF CHEMISTRY

www.rsc.org/materialsA

# Journal Name

## ARTICLE

## Ferroelastic Domains Improve Photochemical Reactivity: A Comparative Study of Monoclinic and Tetragonal $(Bi_{1-0.5x}Na_{0.5x})(V_{1-x}Mo_x)O_4$ Ceramics

Ratiporn Munprom, Paul A. Salvador, and Gregory S. Rohrer*

The relative reactivities of monoclinic and tetragonal $BiVO_4$-based ceramics are described, focusing on the contributions of ferroelastic domains and surface orientations. First, the photo-oxidation of $Mn^{2+}$ on monoclinic $BiVO_4$ is shown to be domain selective, occurring on the set of domains that is not active for the photo-reduction of $Ag^+$. Next, the domain and orientation dependent photochemical reduction of $Ag^+$ is investigated for two samples in the co-doped family $(Bi_{1-0.5x}Na_{0.5x})(V_{1-x}Mo_x)O_4$: a monoclinic sample (x = 0.05) and a tetragonal sample (x = 0.175). Like $BiVO_4$, the x = 0.05 sample has ferroelastic domains that exhibit contrast in piezoresponse force microscopy (PFM) and exhibit domain specific reactivity. The x = 0.175 sample has no domains, no PFM contrast, and uniform grain reactivity. The orientation dependence of $Ag^+$ reduction is similar for the two samples, with surfaces near (001) being more active than others. For any given orientation, however, the monoclinic sample is quantitatively more active than the same orientation in the tetragonal sample. These collected results are consistent with the hypothesis that monoclinic-structured $BiVO_4$ ceramics have enhanced photochemical activity owing to ferroelastic domain-selective reactivity, which allows for local separation of photogenerated carriers and redox reactions.

## 1. Introduction

Solar fuel technologies aim to generate chemical fuels, such as $H_2$, using solar energy. Photocatalytic water splitting is one example of a solar fuel technology, where a photocatalyst absorbs light and uses that energy to split water into $H_2$ and $O_2$. In general, this photocatalytic process is composed of three sequential steps: (1) light absorption, (2) charge transport, and (3) surface reactions.[1,2] An ideal photocatalyst should: (i) absorb a significant portion of the incident light spectrum, generating a large population of charge carriers; (ii) have active surface states for redox reactions, minimizing activation or concentration overpotentials;[2] and (iii) separate the charge carriers to the surface reaction sites, avoiding recombination.[3] This paper is concerned with the charge separation issue, focusing on a known visible light absorbing photocatalyst, $BiVO_4$. $BiVO_4$ is well known for its high photocatalytic efficiency for water oxidation,[4–6] strong absorption in the visible region of spectrum,[7,8] chemical stability in photochemical reactions,[9–11] and relatively low cost.[12,13] However, photo-generated electron-hole recombination is reported to limit the performance of $BiVO_4$.[14]

Internal fields in photocatalysts are integral to charge separation, arising from surface terminations and ferroelectric phenomena in single-phase materials, and polymorph or p–n junctions in multi-phase samples.[15] Some of these methods have already been used to introduce internal fields in $BiVO_4$. For example, heterojunctions between $Co_3O_4$ and $BiVO_4$ have shown notable improvements in the rate of oxidation reactions.[16–19] Surface orientation differences also impact the overall activity in $BiVO_4$ for water oxidation[20] and control the spatial selectivity of photochemical marker reactions.[4,21–23] In marker reaction experiments, reduction appears favored on (001) surfaces and oxidation appears favored on surfaces away from the (001).[20–23] While the origin of these observations can be associated with different internal fields at or between different facets,[4,20–23] other factors are known to affect the reactivity and it is generally thought that a single simple parameter might not be sufficient to describe the orientation dependence of the reactions.[4] Whatever the origin, it is important to consider the orientation of the surface when comparing the reactivity of different samples.

In ferroelectrics, domains of different polarization states intersect surfaces and exhibit different photochemical activities. Domains with positive surfaces attract electrons and promote photo-reduction, while domains with negative surfaces attract holes and promote photo-oxidation.[15,24] The ferroelectric contribution to surface reactivity can modulate or even overwhelm orientation dependent reactivity differences.[25,26] Unfortunately, most ferroelectrics have wide

* Department of Materials Science and Engineering, Carnegie Mellon University, 5000 Forbes Ave., Pittsburgh, PA 15213-3890, USA.
E-mail: gr20@andrew.cmu.edu

band gaps that do not absorb significant portions of the solar spectrum. The narrow gap ferroelectric $BiFeO_3$ exhibits domain selective reactivity when illuminated with visible light.[27] Recently, we discovered that the centrosymmetric ferroelastic monoclinic $BiVO_4$ also exhibits spatially selective visible light stimulated surface photoreactivity that correlates to the ferroelastic domain structure.[28] Moreover, the domains generate contrast in piezoresponse force microscopy (PFM) that correlates to the reactivity, exactly like polar domains in ferroelectrics, yet polarity is not a bulk property of centrosymmetric crystals.[28] The implication is that the ferroelastic domains in monoclinic $BiVO_4$ have internal fields capable of improved charge separation and reduced recombination.[14] Although domain specificity has been observed for both oxidation and reduction reactions on $BiVO_4$,[21] it has not yet been shown that oxidation and reduction occur on distinct subsets of the domains, a property we refer to here as "complementarity." Moreover, it remains to be demonstrated if the ferroelastic domains lead to improved reactivity.

Our approach to investigating these questions is to directly demonstrate the complementarity of domain reactivity on monoclinic $BiVO_4$, using marker reactions.[21,23,28] To investigate whether ferroelasticity leads to improved reactivity, we compare the reactivity of monoclinic (ferroelastic) and tetragonal (non-ferroelastic) $BiVO_4$-based samples with similar surface orientations, over all of orientation space. The stable phase of $BiVO_4$ at room temperature is monoclinic.[29] The ferroelastic transformation from the high-temperature tetragonal phase to the low-temperature monoclinic phase occurs at 255 °C. This transformation temperature can be suppressed by co-doping in the $(Bi_{1-0.5x}Na_{0.5x})(V_{1-x}Mo_x)O_4$ family, where the tetragonal structure is maintained to room temperature for $x \geq 0.10$.[30] Therefore, we fabricated and compared the reactivity for a monoclinic x = 0.05 sample and a tetragonal x = 0.175 sample, focusing on comparing whether domain specific reactivity is observed and if quantitative differences in the overall reactivity could be observed for comparable orientations.

## 2. Experimental

Monoclinic (x= 0 and 0.05) and tetragonal (x = 0.175) samples of $(Bi_{1-0.5x}Na_{0.5x})(V_{1-x}Mo_x)O_4$ were synthesized by solid-state reaction. Stoichiometric ratios of $Bi_2O_3$, $V_2O_5$, $NaCO_3$, and $MoO_3$ were mixed and then wet ball-milled in ethanol for 24 hours using YSZ as a grinding media. The mixed powder was then put in a drying oven at 80 °C to remove the ethanol, and the dried powder was calcined at 600 °C for 3 hours. The powder was manually reground and calcined several times to obtain fine powders, and the calcined powders were characterized by x-ray diffraction (XRD) to confirm full reaction to the targeted structures. Then, a few drops of PVA was mixed manually with 1 g of fine powder, and the mixture was pressed into a 1 cm-diameter cylindrical-shaped pellet using a hydraulic pressure of 6 metric tons. The green pellet was heated at 500 °C for two hours, to remove the PVA, and was

then annealed at 780 °C for 20 hours to obtain a dense sintered ceramic. The surfaces of the obtained ceramics were lapped and polished with SiC papers, followed by polishing with successively finer $Al_2O_3$ polishing suspensions, until mirror-like surfaces were obtained. Afterwards, the samples were annealed at 300 °C for 1 hour to heal surface damage from the polishing. The polished samples were also measured for their order-of-magnitude electronic conductivity using the van der Pauw technique at room temperature.

All samples were used to photochemically reduce $Ag^+$. An O-ring was placed on the surface of the specimen and then filled with 0.115 M $AgNO_3$ aqueous solution. A quartz slip was put on top of the O-ring(s) to create a flat and uniform surface for illumination. The undoped sample was tested and illuminated alone. The co-doped samples were tested and illuminated together to remove the possibility that differences in reactivity of the two samples were related to changes in the experimental conditions. Each was placed in an O-ring filled with an identical solution environment, placed adjacent to each other in the center of the illuminated region, and then covered with the same quartz. Samples were illuminated from the topside using a blue LED ( $\lambda_{peak}$ = 470 nm, Philips Lumileds, San Jose, CA), and the set-up was arranged to optimize examination of the initial reactivity using atomic force microscopy (AFM). For the undoped sample, the light source was in contact with the quartz slip, the power was 330 mW (0.75 A and 0.44 V), and the exposure time was 60 s (consistent with our previous studies[21,28]). For the co-doped samples (which were more reactive), the light source was ~ 1 cm above the cover slip, the power was 220 mW (0.5 A and 0.44 V), and the exposure time was 10 or 30 s. After exposure, the sample was rinsed in water to avoid the precipitation of residual $AgNO_3$ and then dried. For the undoped $BiVO_4$, the photochemical oxidation of $Mn^{2+}$ was investigated on the same area where $Ag^+$ reduction was observed, using identical illumination conditions and a 0.115 M $MnSO_4$ aqueous solution containing $NaIO_3$ as an electron acceptor. Prior to the oxidation experiment, silver deposits were wiped from the sample surface, and the sample was cleaned in an ultrasonic bath of methanol and then acetone, for 5 min each.

After reaction, the surface topography of the samples was imaged using AFM[31] and scanning electron microscopy (SEM). The heights of deposits were measured on 50 grains, and these were used to classify the relative reactivity of each co-doped sample. To obtain the relationship between reactivity and orientation, the surface orientations of grains were quantified using electron backscatter diffraction (EBSD) in a Quanta200 SEM (FEI, Hillsboro, Oregon) equipped with an orientation imaging microscopy (OIM) system. For the co-doped samples, the orientations were measured in a 100 μm x 100 μm area, using a scan step of 0.1 μm. EBSD patterns were automatically collected and indexed by the TSL software.[21] Indexing was carried out using a tetragonal unit cell in the Laue group 4/m with $a = b$ = 5.1509 Å and $c$ = 11.73 Å, for both the monoclinic and tetragonal samples. The co-doped monoclinic system can be indexed as tetragonal because the distortion between $a$ and $b$ is only 2 % and γ is very close to 90° (as described

previously[21]). The raw orientation data was cleaned using procedures in the TSL software,[21] including grain dilation (using 5 °), a grain orientation averaging (using 5 °), and a pseudo symmetry correction (for misorientations of 90 ° around (001) axis). Grains were classified as either being high or low reactivity (the quantitative criteria for these distinctions are described later), and the relative reactivity was plotted as a function of orientation using a stereographic projection.

## 3. Results

AFM topography images from the same area of an undoped monoclinic $BiVO_4$ sample after the photochemical reduction of $Ag^+$ (Fig. 1(a)) and oxidation of $Mn^{2+}$ (Fig. 1(b)) are shown in Fig. 1. After reaction, insoluble particles were found on the surface and appear as bright contrast in the AFM images. The reactivity observed in Fig. 1(a) is similar to the initial report that the surface of undoped $BiVO_4$ exhibits domain-specific reactivity for the photochemical reduction $Ag^+$.[28] The reactivity observed in Fig. 1(b) indicates that the photochemical oxidation of $Mn^{2+}$ also occurs in a domain selective fashion. Moreover, a comparison of the two images (focusing on the central grain) reveals that the reactions occur on complementary sets of domains: domains active for reduction alternate with those active for oxidation, and domains active for one reaction are not active for the other. This alternation leads to a spatial separation of the redox reactions over the surface of an individual grain in this non-polar, centrosymmetric material. This observation confirms that the behavior of these ferroelastic domains is similar to ferroelectric domains in other known photocatalysts.[24,32] The separation of the reduction and oxidation reactions shows the potential of the ferroelastic domains to reduce the recombination of the electron-hole pairs and, thus, possibly increase the overall efficiency. In addition, this result reveals the ability of both reduction and oxidation reactions to happen on the same surface orientation.
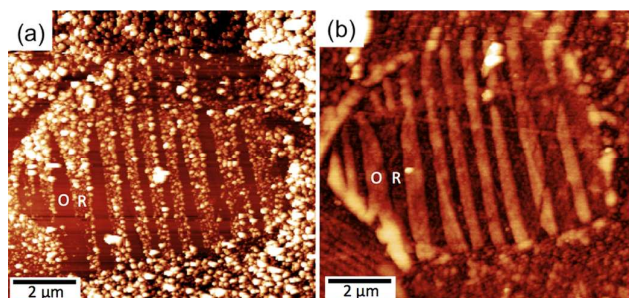


Fig. 1: Surface topography after (a) $Ag^+$ reduction and (b) $Mn^{2+}$ oxidation. The images are taken on the same area. The vertical scale is 80 nm and 150 nm for (a) and (b), respectively. 'O' indicates a domain that promotes oxidation and 'R' indicates a domain that promotes reduction.

To test the hypothesis that the ferroelastic domain structure can enhance the overall photochemical reactivity, the orientation and domain dependent reactivities of two compositions in the co-doped $(Bi_{1-0.5x}Na_{0.5x})(V_{1-x}Mo_x)O_4$ family were compared: one composition with a monoclinic structure (x = 0.05) and the other with a tetragonal structure (x = 0.175).

The two samples were initially characterized by XRD. The diffraction patterns (see Fig. S1) were consistent with expectations:[30] the x = 0.05 sample was monoclinic and the x = 0.175 sample was tetragonal. The ferroelastic domain structure of the polished samples was then investigated. SEM micrographs, recorded using back-scattered electron (BSE) contrast, are shown in Fig. 2(a) and 2(b) for the x = 0.05 and x = 0.175 samples, respectively. BSE contrast is sensitive to ferroelastic domains, which gives rise to the striped patterns inside grains for the monoclinic ferroelastic composition (Fig. 2(a)). As expected, no domains can be observed for the tetragonal sample (Fig. 2(b)).

The electrical resistivities of the samples were measured. The co-doped samples had similar resistivities of $\approx 10^6$ Ω-cm, while the resistivity of the undoped sample was at least (it was too resistive to measure) two orders of magnitude greater at > $10^8$ Ω-cm.[33] Co-doping according to the stoichiometry $(Bi_{1-0.5x}Na_{0.5x})(V_{1-x}Mo_x)O_4$ is, ideally, self-compensating: no changes in other defect populations, such as electronic carriers, is required. Nevertheless, the doped samples had conductivities similar to each other and at least 100 times greater than the undoped sample. To avoid complications in interpreting reactivity differences arising from differences in conductivity, we focused on comparing the photochemical reactivity of the co-doped samples of different symmetry but similar conductivity.

In prior work on $BiVO_4$,[28] the domain selectivity for $Ag^+$ reduction was correlated more strongly to the piezoresponsive nature of domains (measured using PFM) than the surface topography (imaged using AFM). To explore whether surfaces in the $(Bi_{1-0.5x}Na_{0.5x})(V_{1-x}Mo_x)O_4$ family were piezoresponsive, we carried out PFM investigations of the two co-doped samples. The surface topography (plotted as the error signal) of the two co-doped samples are shown in Fig. 3(a) and (c), respectively for the monoclinic and tetragonal samples. The piezoresponses (plotted as the phase signal) from the same areas are given in Fig 3(b) and 3(d), for the monoclinic and tetragonal samples, respectively. In the topographic images, contrast arising from grain boundaries and polishing scratches are clearly observed in both samples. However, contrast arising from ferroelastic domains is observed only for the co-doped monoclinic sample, corresponding to narrow parallel lines within a given grain. In the PFM phase images, weak contrast is observed in both samples from grain boundaries, but strong contrast correlated to domains is observed only in the monoclinic sample. These results indicate that the co-doped monoclinic x = 0.05 sample is similar to undoped monoclinic $BiVO_4$,[28] both monoclinic samples having piezoresponsive (polar) ferroelastic domains at their surfaces (these samples are directly compared in Fig. S2). The co-doped tetragonal sample, however, does not have ferroelastic domains and has no clear piezoresponsive regions at the surface.
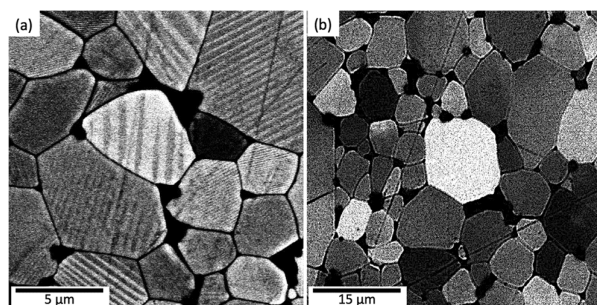
Fig. 2: SEM micrographs (BSE contrast) of (a) co-doped monoclinic (x = 0.05), and (b) co-doped tetragonal (x = 0.175) $(Bi_{1-0.5x}Na_{0.5x})(V_{1-x}Mo_x)O_4$.

Example AFM topographs after photochemical reduction of $Ag^+$ (using a 30 s exposure) are given in Fig. 4(a) and (d) for the monoclinic x = 0.05 and tetragonal x = 0.175 sample, respectively. Silver deposits were found on the surfaces of both co-doped samples, though the amount of silver varied from grain to grain. This is consistent with an orientation dependent reactivity, similar to that reported for the undoped $BiVO_4$ sample.[21] The local surface orientation, determined using EBSD, from these same areas is shown in Fig. 4(b) and (e) for the x = 0.05 and 0.175 samples, respectively. The topographic height profiles of deposits along the dashed lines in Fig. 4(a) and 4(d) are shown in Fig 4(c) and 4(f), respectively. We used these height variations to quantify the relative reactivity for grains within each sample. Because the deposition rates on the co-doped monoclinic and co-doped tetragonal samples are different, the criteria for classifying the reactivity for both samples are also different. For the co-doped x = 0.05 monoclinic sample, the deposit heights were generally higher, so grains with deposits greater (less) than 20 nm in average height were classified as having high (low) reactivity. For the co-doped x = 0.175 sample the average deposit heights were generally lower, and grains with deposits greater (less) than 10 nm height were classified as having high (low) reactivity. The lines in Fig. 4(a) and (d) were chosen such that they traversed grains classified as having high reactivities (H in the images) and low reactivities (L in the images), for both samples. It should be noted here that, for the surfaces on the monoclinic sample classified as low reactivity, such as the grain marked L in the lower left of the image, the spatial distribution is reminiscent of the ferroelastic domains. No domains were observed on the tetragonal sample. We will return to the domain specificity later.

More than 50 grains in each sample were characterized for their relative reactivity and orientation. The relative reactivity is plotted as a function of orientation (in the standard stereographic projection for the tetragonal reference frame[21]) in Fig. 5(a) and 5(b) for the x = 0.05 monoclinic and x = 0.175 tetragonal samples, respectively. Despite the somewhat subjective distinction between H and L reactive grains in the two samples, (001)-oriented grains were observed to be more highly reactive than others: as the angle between the surface orientation and [001] increases, there are fewer grains whose average heights of silver particles exceed 20 nm for the x =

0.05 (10 nm for x = 0.175) sample. These results are also consistent with the orientation-dependent reactivity observed for undoped $BiVO_4$.[21] The photo-deposition on these co-doped samples was generally higher than for the undoped sample, even with a shorter exposure time, a lower power of illumination, and a larger distance between the light source and samples, which all should decrease the reactivity[21]. It is possible that the higher electronic conductivity of the doped samples contributes to their higher reactivities.[34,35]
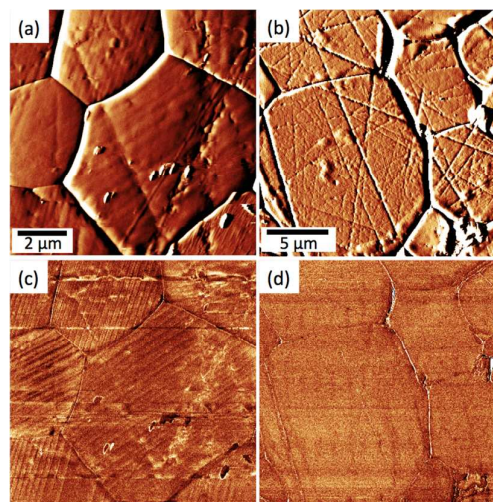


Fig. 3: Topographic AFM images of (a) monoclinic x = 0.05 and (c) tetragonal x = 0.175 $(Bi_{1-0.5x}Na_{0.5x})(V_{1-x}Mo_x)O_4$, each plotted as error signals with a vertical scale of 0.2 nA. (b) and (d) are PFM phase images from the same areas as given in (a) and (c), respectively. The range of the vertical scale for the PFM images ((b) and (d)) is 2.4°.

Figure 6 shows similar results to those of Fig. 4, but in areas selected to compare the reactivities of monoclinic and tetragonal grains with nearly identical orientations. AFM topographs after the photochemical reduction of $Ag^+$ (orientations maps) are given in Fig. 6(a) and (d) (Fig. 6(b) and (e)) for the monoclinic and tetragonal sample, respectively. The height profiles along the dashed lines in Fig. 6(a) and 6(d) are shown in Fig 6(c) and 6(f), respectively. The lines in Fig. 6(a) and (d) were chosen such that they remained within grains of similar orientations indexed in the tetragonal reference frame (marked with * in (b) and (e)). The small distortions from the tetragonal structure for the x = 0.05 sample will not significantly impact this analysis. The height of deposits on the monoclinic grain, see Fig. 6(c), was greater than the height of those on the tetragonal grain of the same orientation, see Fig. 6(d). In fact, when we compare the relative reactivities of grains of similar orientations (eight pairs), the reactivity the x = 0.05 monoclinic grains was always greater than that of the x = 0.175 tetragonal grains (the orientations and the measured reactivity of all compared grains are shown in Fig. S3). These results support the conclusion that the monoclinic sample is more reactive than the tetragonal sample.
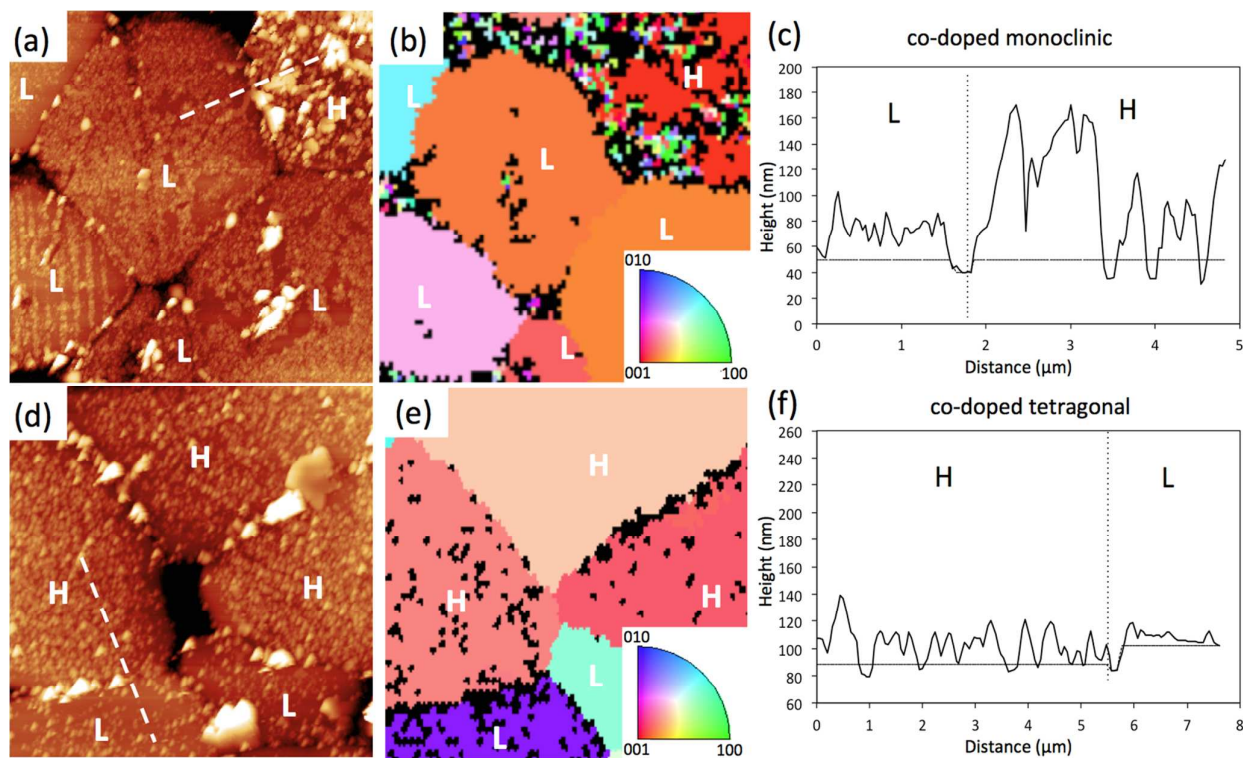
Fig. 4: Surface topographic images taken after the reduction of $Ag^+$ for 30 s on the surface of (a) the x = 0.05 monoclinic sample and (d) the x = 0.175 tetragonal sample. Inverse pole figure (orientation) maps from the same areas are shown in (b) and (e), respectively. Pixels with low confidence indices are colored black. Topographic line profiles from the dashed lines in (a) and (d) are shown in (c) and (f), respectively. The vertical (horizontal) lines in (c) and (f) mark the grain boundary (height of bare grain surface). In all images, symbols denote grains of relatively high (H) or low (L) reactivities (see text).
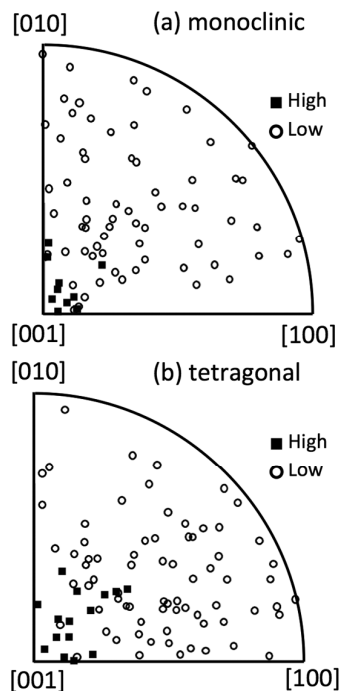


Fig. 5: Orientation distribution of grains with high and low reactivity in (a) co-doped x = 0.05 monoclinic and (b) co-doped x = 0.175 tetragonal $(Bi_{1-0.5x}Na_{0.5x})(V_{1-x}Mo_x)O_4$.

In Fig. 6(a), domain selective reactivity is clearly observed for several grains in the x = 0.05 monoclinic sample, but not for the tetragonal sample. In fact, domain-to-domain variation was generally observed for the monoclinic co-doped sample, when the reactivity of the grain was low (L). In highly reactive grains, $Ag^+$ generally coated the entire grain, presumably from lateral growth on the surface of previously nucleated silver deposits. The domain-selective reactivity in monoclinic co-doped $(Bi_{1-0.5x}Na_{0.5x})(V_{1-x}Mo_x)O_4$ is similar to that previously reported for undoped $BiVO_4$.[28] This indicates that the domain-specific spatially-selective reactivity of fergusonite-structured $BiVO_4$ is not restricted to a specific composition (see Fig. S2 for a comparison of PFM for the two monoclinic samples, and see Fig. S4 for one-to-one correlation between PFM domains and photoreduction of $Ag^+$ on the x = 0.05 sample). Furthermore, the increased conductivity of the x = 0.05 sample appears to render the co-doped sample more reactive than the undoped sample. In a previous study of domain specific reactivity on $TiO_2$ supported on $BaTiO_3$, increasing the carrier concentration led to spatially uniform reactivity, presumably because the additional donors screened the polarization of the domains.[25] That does not seem to be the case for the surface of $(Bi_{1-0.5x}Na_{0.5x})(V_{1-x}Mo_x)O_4$.
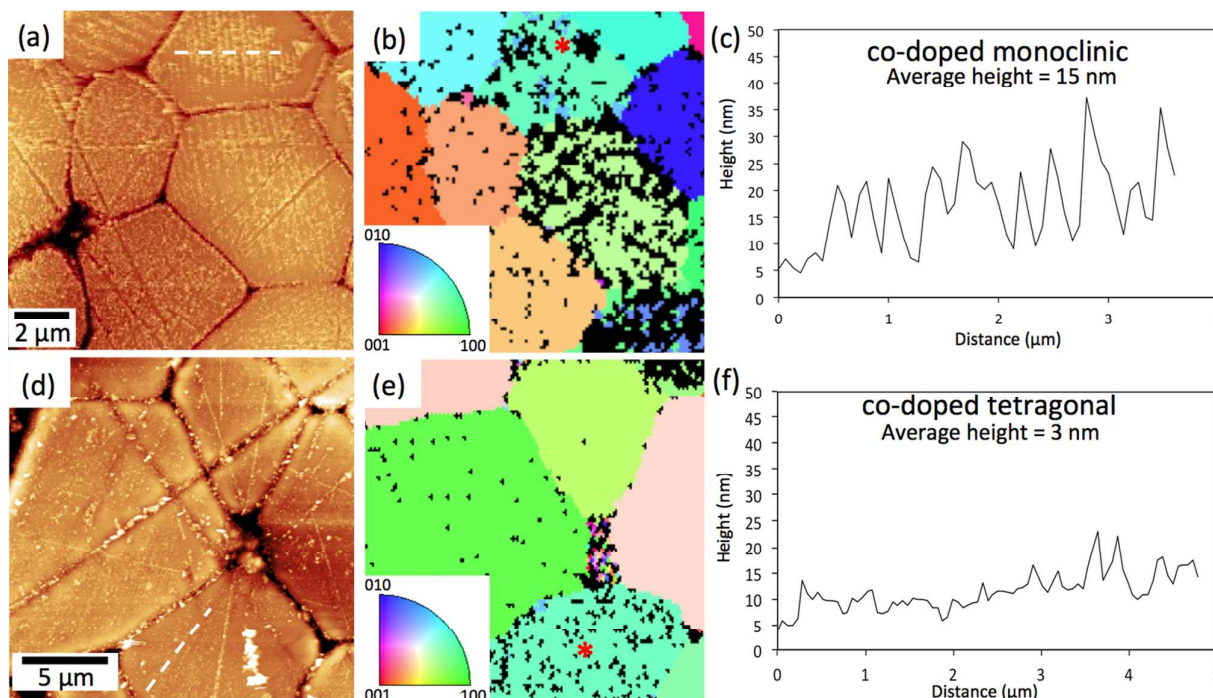
Fig. 6: Surface topographic images of (a) the x = 0.05 monoclinic sample and (d) the x = 0.175 tetragonal sample of $(Bi_{1-0.5x}Na_{0.5x})(V_{1-x}Mo_x)O_4$ after a 10 s $Ag^+$ reduction. Orientation maps of the same areas are shown in (b) and (e), respectively. Pixels with low confidence indices are colored black . Topographic line profiles from the dashed lines in (a) and (d), from the grains marked with * in (b) and (e), are shown in (c) and (f), respectively.

## Discussion

Despite their different room temperature crystal symmetries, the orientation-dependent reactivities observed for the co-doped monoclinic and tetragonal samples are essentially the same: surfaces near (001) are more reactive than others for the photochemical reduction of $Ag^+$. A similar orientation dependent reactivity was observed for undoped monoclinic $BiVO_4$.[21] These results indicate that the orientation dependent reactivity is closely tied to the structure (and bonding) of the parent tetragonal scheelite phase, and that the small distortions leading to the monoclinic phase do not markedly influence orientation-dependent behavior. However, the monoclinic co-doped sample was found to be more active on any given orientation than was the tetragonal co-doped sample, which is consistent with prior studies indicating that the monoclinic phase of $BiVO_4$ is more active than the tetragonal phase.[8,36–38] That the increased photo-reactivity of monoclinic $BiVO_4$ arises for every orientation indicates orientation effects are not the origin of this improvement.

Prior explanations of the better photocatalytic performance of monoclinic $BiVO_4$ over tetragonal $BiVO_4$ have been attributed to two factors associated with the monoclinic distortion: the appearance of local polarizations in the metal-oxygen environments and a change in the average electronic structure related to the changes in metal-oxygen bonding. In the tetragonal scheelite structure, the metal oxygen polyhedra are symmetric, with the cations at the center of the polyhedra. In the monoclinic fergusonite structure (sometimes called the monoclinic scheelite structure), the polyhedra are distorted and the cations are off-centered within them.[36] This results in local polar units in fergusonite, while the net polarity is zero when all summed over the entire centrosymmetric unit cell. Tokunaga et al.[36] proposed that these local polarizations result in a significant improvement of charge separation, and thereby enhance the reactivity of monoclinic $BiVO_4$. It is likely that these local polar units do not completely cancel at the surfaces of $BiVO_4$, where symmetry is broken, which is essentially what we measure in the PFM images that demonstrate net surface polarity in monoclinic $BiVO_4$, but not in tetragonal $BiVO_4$. That the local distortions differ near the surface was implied in Raman signals measured using different laser wavelengths.[39]

The electronic structure also changes as a result of the monoclinic distortion in $BiVO_4$, because it is directly coupled to the metal-oxygen bonding environments.[40] In $BiVO_4$, the Bi 6s lone pair is stereochemically inactive in the symmetric Bi-O environment of the tetragonal scheelite structure, but is active in the distorted environment of the monoclinic fergusonite structure.[38] When the lone-pair becomes active, it hybridizes with the valence band oxygen, contributing significantly to the valence band edge.[7,37,38,40–42] Concomitantly, the distortion of the V-O tetrahedra modifies the conduction band states (which are primarily V orbitals). Experimentally, there is little difference in the absorption edges of tetragonal scheelite and monoclinic fergusonite $BiVO_4$ (though a relatively large shift

occurs on massive structural change to the tetragonal zircon-structured BiVO$_4$).[36,39,42,43] Therefore, there is little change to the amount of light absorbed. However, these hybridizations are believed to increase the electron and hole mobilities, which therefore improve the performance of the photocatalysts as electron and holes are more easily separated.[44] We cannot determine the role that the improved hybridization of the band edge states in the monoclinic systems played in our observations. However, whatever the role, it cannot explain the orientation-dependent reactivity of the two doped samples. It can, however, contribute to a possible improved performance for a given reaction occurring on a specific ferroelastic domain, when compared to the same reaction occurring on a similarly oriented tetragonal grain.

What prior investigations have not considered is the role that local surface polarity may play on improved reactivity. Local surface polarity is known to promote charge separation, reduce recombination, and drive electrons and holes to different reaction sites on the surface, which also results in a spatial separation of chemical reactions.[15] Here we demonstrated from PFM measurements that monoclinic co-doped BiVO$_4$ exhibits regions of varying surface polarization, similar to that reported for undoped monoclinic BiVO$_4$.[28] Moreover, the reduction of Ag$^+$ on the surface of the co-doped monoclinic material is spatially correlated to domains (and can be correlated to the PFM signal from domains), as reported for the undoped material.[21,36] We also show that complementary redox reactions occur on complementary sets of domains (Fig. 1). This indicates that the existence of locally polar polyhedra in the centrosymmetric bulk are not the primary driver for improved performance, but that net, non-zero polar domains at the surface drive the spatial separation of electrons and holes, and therefore the separation of photochemical reactions.

In addition to the increased reactivity, the co-existence of complementary ferroelastic domains on all grains also provides sites for both reduction and oxidation on all surfaces. This makes it possible for both reduction and oxidation to happen on any orientation, which has not been observed in the previous study of polygonal BiVO$_4$.[23] We conclude that the existence local surface polarity separated into complementary domain patterns, which do not exist in the tetragonal (Bi$_{1-0.5x}$Na$_{0.5x}$)(V$_{1-x}$Mo$_x$)O$_4$, leads to the increased reactivity in monoclinic (Bi$_{1-0.5x}$Na$_{0.5x}$)(V$_{1-x}$Mo$_x$)O$_4$. While some additional benefit may arise from improved mobilities associated with the increased hybridization, the results suggest that the primary factor that increases the photocatalytic performance of monoclinic (Bi$_{1-0.5x}$Na$_{0.5x}$)(V$_{1-x}$Mo$_x$)O$_4$ is the existence of complementary sets of polar ferroelastic domains.

Increased reactivities arising from spatially varying polar domains of opposite signs are commonly seen in ferroelectrics, which possess inherently non-centrosymmtric structures.[27,45–47] One does not anticipate such effects in centrosymmetric structures, for which a net internal polarization is forbidden. We have previously argued that the non-zero polarizations measured at the surface of centrosymmetric BiVO$_4$ arise from flexoelectric effects.[28] Flexoelectricity is defined as a linear relationship between an electric field and a strain gradient, where the strain gradient breaks the symmetry, resulting in a local polarization. Thus, flexoelectricity is not limited to non-centrosymmetric materials.[48,49] The contribution of the polar nature of ferroelectric surfaces has been shown to spatially promote the separation of charge carriers and therefore increase reactivity in many studies.[15,24,26,50–52] Similarly, the increased reactivity of our monoclinic BiVO$_4$ samples can be attributed by the induced polar nature of surfaces from flexoelectricity, which appears to be coupled to specific sets of ferroelastic domains.

Because we varied the composition to stabilize the monoclinic and tetragonal phases of (Bi$_{1-0.5x}$Na$_{0.5x}$)(V$_{1-x}$Mo$_x$)O$_4$, we need to consider chemical effects as well. For example, the materials studied here all have slightly different colors: undoped BiVO$_4$ is a bright shade of yellow, the x = 0.05 sample is light yellow and the x = 0.175 sample is darker yellow. However, it has already been established by Zhou et al.[30] that the band gaps of these two compositions of (Bi$_{1-0.5x}$Na$_{0.5x}$)(V$_{1-x}$Mo$_x$)O$_4$ are comparable, indicating that they absorb approximately the same amount of light. Also, because we used narrow band illumination far from the band edge, a small shift in the band edge will not have a significant effect on the amount of light absorbed. Thus, differences in light absorption are not likely to be responsible for the differences in reactivity.

The conductivity also varies with composition, either from changes in carrier populations or mobilities. Abdi et al.[34] demonstrated that doping BiVO$_4$ with W increased the conductivity, which resulted in higher carrier mobility, and therefore better photocatalytic performance. Our co-doped samples have higher conductivities (by at least two orders of magnitude) than the undoped sample, but are similar to each other. The increased conductivity of the co-doped samples explains their improved reactivity when compared to the undoped sample, but does not provide a satisfactory description for the differences in reactivity observed between the doped samples. Also, the fact that both reduction and oxidation reactions can occur on any surface orientation of the sintered ceramic sample, but not the small polygonal crystals,[23] suggests that the co-existence of regions promoting oxidation and reduction on each surface improves the reactivity by promoting local charge separation and balancing the local rates of both redox reactions.

## Conclusions

Complementary, domain-specific, reduction and oxidation reactions were observed on the surface of a ferroelastic monoclinic BiVO$_4$ ceramic. It suggests that surface polarizations correlated with the ferroelastic domain structure controls photogenerated charge separation. A study of the orientation dependence of the photochemical reactivity of co-doped monoclinic and tetragonal (Bi$_{1-0.5x}$Na$_{0.5x}$)(V$_{1-x}$Mo$_x$)O$_4$ showed that, for the reduction of silver, the most reactive orientation was (001) in both materials. Even though the orientation dependence of the reactivity was comparable for

the two different compositions of $(Bi_{1-0.5x}Na_{0.5x})(V_{1-x}Mo_x)O_4$, the photochemical reactivity of the monoclinic composition was greater than that of the tetragonal composition. The enhanced photochemical reactivity of the monoclinic sample is most likely caused by the ferroelastic domain structure, which leads to surface polarization measured using PFM. It is therefore likely that the improved photochemical reactivity of the monoclinic ferroelastic material arises from polar domains that transport electrons and holes to the surfaces of different domains, providing spatially distinct sites for oxidation and reduction.

## Acknowledgements

## Notes and references

1 K. Maeda and K. Domen, *J. Phys. Chem. C*, 2007, **111,** 7851–7861.
2 R. M. Navarro Yerga, M. C. Álvarez Galván, F. del Valle, J. A. Villoria de la Mano and J. L. G. Fierro, *ChemSusChem*, 2009, **2,** 471–485.
3 A. Kudo, *Int. J. Hydrog. Energy,* 2006, **31,** 197–202.
4 J. Yang, D. Wang, X. Zhou and C. Li, *Chem. Weinh. Bergstr. Ger.*, 2013, **19,** 1320–1326.
5 Y. Park, K. J. McDonald and K.-S. Choi, *Chem. Soc. Rev.*, 2013, **42,** 2321–2337 .
6 Z.-F. Huang, L. Pan, J.-J. Zou, X. Zhang and L. Wang, *Nanoscale,* 2014, **6,** 14044–14063.
7 A. Walsh, Y. Yan, M. N. Huda, M. M. Al-Jassim and S.-H. Wei, *Chem. Mater.*, 2009, **21,** 547–551.
8 H. Fan, T. Jiang, H. Li, D. Wang, L. Wang, J. Zhai, D. He, P. Wang and T. Xie, *J. Phys. Chem. C*, 2012, **116,** 2425–2430.
9 Z. Ge, C. G. Dosoretz and Z. He, *Desalination*, 2014, **341,** 101–106.
10 J. A. Seabold and K.-S. Choi, *J. Am. Chem. Soc.*, 2012, **134,** 2186–2192.
11 M. T. McDowell, M. F. Lichterman, J. M. Spurgeon, S. Hu, I. D. Sharp, B. S. Brunschwig and N. S. Lewis, *J. Phys. Chem. C,* 2014, **118**, 19618–19624.
12 M. Zhong, T. Hisatomi, Y. Kuang, J. Zhao, M. Liu, A. Iwase, Q. Jia, H. Nishiyama, T. Minegishi, M. Nakabayashi, N. Shibata, R. Niishiro, C. Katayama, H. Shibano, M. Katayama, A. Kudo, T. Yamada and K. Domen, *J. Am. Chem. Soc.*, 2015, **137**, 5053–5060.
13 X. Yang, R. Liu, Y. He, J. Thorne, Z. Zheng and D. Wang, *Nano Res.*, 2014, **8,** 56–81.
14 Y. Ma, S. R. Pendlebury, A. Reynal, F. Le Formal and J. R. Durrant, *Chem. Sci.*, 2014, **5,** 2964–2973.
15 L. Li, P. A. Salvador and G. S. Rohrer, *Nanoscale*, 2013, **6,** 24–42.
16 F. F. Abdi, N. Firet and R. van de Krol, *ChemCatChem*, 2013 **5,** 490–496.
17 M. Long, W. Cai, J. Cai, B. Zhou, X. Chai and Y. Wu, *J. Phys. Chem. B*, 2006, **110**, 20211–20216.
18 C. Long and H. Kisch, *J. Phys. Chem. C* , 2008, **112,** 548–554.
19 J. Wang and F. E. Osterloh, *J. Mater. Chem. A*, 2014, **2,** 9405–9411.
20 D. Wang, H. Jiang, X. Zong, Q. Xu, Y. Ma, G. Li and C. Li, *Chem. – Eur. J.*, 2011, **17,** 1275–1282.
21 R. Munprom, P. A. Salvador and G. S. Rohrer, *J. Mater. Chem. A*, 2015, **3,** 2370–2377.
22 R. Li, H. Han, F. Zhang, D. Wang and C. Li, *Energy Environ. Sci.*, 2014, **7,** 1369–1376.
23 R. Li, F. Zhang, D. Wang, J. Yang, M. Li, J. Zhu, X. Zhou, H. Han and C. Li, *Nat. Commun.*, 2013, **4**, 1432.
24 J. L. Gioconodi and G. S. Rohrer, *J. Phys. Chem. B*, 2001, **105,** 8275–8277.
25 N. V.Burbure, P. A. Salvador and G. S. Rohrer, *Chem. Mater.*, 2010, **22,** 5823–5830.
26 N. V.Burbure, P. A. Salvador and G. S. Rohrer, *Chem. Mater.*, 2010, **22,** 5831–5837.
27 A. M.Schultz, Y. Zhang, P. A. Salvador and G. S. Rohrer, *ACS Appl. Mater. Interfaces*, 2011, **3,** 1562–1567.
28 R. Munprom, P. A. Salvador and G. S. Rohrer, *Chem. Mater.,* 2014, **26,** 2774–2776.
29 W. I. F. David, A. M. Glazer and A. W. Hewat, *Phase Transit.*, 1979, **1,** 155–169.
30 D. Zhou, L.-X. Pang, H. Wang, J. Guo, X. Yao and C. A. Randall, *J. Mater. Chem.*, 2011, **21,** 18412–18420.
31 J. A. Last, P. Russell, P. F. Nealey and C. J. Murphy, *Invest. Ophthalmol. Vis. Sci.*, 2010, **51,** 6083–6094.
32 S. V. Kalinin, D. A. Bonnell, T. Alvarez, X. Lei, Z. Hu, J. H. Ferris, Q. Zhang and S. Dunn, *Nano Lett.*, 2002, **2,** 589–593.
33 A. J. E. Rettie, H. C. Lee, L. G. Marshall, J.-F. Lin, C. Capan, J. Lindemuth, J. S. McCloy, J. Zhou, A. J. Bard and C. B. Mullins, *J. Am. Chem. Soc.*, 2013, **135,** 11389–11396.
34 F. F. Abdi, T. J. Savenije, M. M. May, B. Dam and R. van de Krol, *J. Phys. Chem. Lett.*, 2013, **4,** 2752–2757.
35 K. P. S. Parmar, H. J. Kang, A. Bist, P. Dua, J. S. Jang and J. S. Lee, *ChemSusChem*, 2012, **5,** 1926–1934.
36 S. Tokunaga, H. Kato and A. Kudo, *Chem. Mater.*, 2001, **13,** 4624–4628.
37 J. Coronado, F. Fresno, M. D. Hernández-Alonso and R. Portela, Springer Science & Business Media, 2013.
38 A. Kudo and S. Hijii, *Chem. Lett.*, 1999, **28,** 1103–1104.
39 J. Yu and A. Kudo, *Adv. Funct. Mater.*, 2006, **16,** 2163–2169.
40 K. E. Kweon and G. S. Hwang, *Phys. Rev. B*, 2012, **86,** 165209.
41 M. W.Stoltzfus, P. M. Woodward, R. Seshadri, J.-H. Klepeis and B. Bursten, *Inorg. Chem.*, 2007, **46,** 3839–3850.
42 G. Li, Y. Bai and W. F. Zhang, *Mater. Chem. Phys.*, 2012, **136,** 930–934.
43 H. M. Zhang, J. B. Liu, H. Wang, W. X. Zhang and H. Yan, *J. Nanoparticle Res.*, 2007, **10,** 767–774.
44 K. E. Kweon and G. S. Hwang, *Phys. Rev. B*, 2013, **87,** 205202.
45 P. S. Halasyamani and K. R. Poeppelmeier, *Chem. Mater.*, 1998, **10,** 2753–2769.
46 T. Jungk, Á. Hoffmann and E. Soergel, in Ferroelectric Crystals for Photonic Applications (eds. Ferraro, D. P., Grilli, D. S. & Natale, D. P. D.) 209–228 (Springer Berlin Heidelberg, 2009).
47 47 H. Zhao, H. Kimura, Q. Yao, L. Guo, Z. Cheng and X. Wang, in *Advances in Ferroelectrics*, ed. A. Peliz-Barranco, InTech, 2012.
48 A. K. Tagantsev, *Phys. Rev. B*, 1986, **34,** 5883–5889.
49 P. V. Yudin and A. K. Tagantsev, *Nanotechnology*, 2013, **24,** 432001.
50 M. Stock and S. Dunn, *J. Phys. Chem. C*, 2012, **116,** 20854–20859.
51 Y. Cui, J. Briscoe, and S. Dunn, *Chem. Mater.*, 2013, **25,** 4215–4223.
52 L. Li, G. R. Rohrer, and P. A. Salvador, *J. Am. Ceram. Soc.*, 2012, **95,** 1414–1420.
53

Journal of Materials Chemistry A Accepted Manuscript